Small-angle X-ray diffraction of Kevlar using synchrotron radiation

David T. Grubb* and Keshav Prasad†
Department of Materials Science and Engineering, Cornell University, Ithaca, NY 14853, USA

and Wade Adams
Wright Patterson Air Force Base, Dayton, Ohio, USA
(Received 6 February 1990; revised 22 April 1990; accepted 18 May 1990)

A synchrotron source of X-rays has been used to obtain high-resolution small-angle X-ray scattering (SAXS) patterns from commercial poly(*p*-phenylene terephthalamide) (Kevlar) fibres. In Kevlar 49, detailed analysis of the equatorial streak, often called the 'void scattering', shows that it comes from the crystals in the fibre and not from any voids. The scattering objects producing the SAXS pattern have the same length, width and orientation distribution as the crystals. In Kevlar 149, there is less scatter overall, a bimodal distribution of sizes and orientation, and an off-axis streak at $\pm 25°$ to the equator. Similar off-axis small-angle scattering has recently been seen in other rigid-rod polymer fibres, but the fibre structure producing it is not understood.

(Keywords: small angle X-ray diffraction; Kevlar; fibres; synchrotron radiation)

INTRODUCTION

In small-angle X-ray scattering (SAXS) practical matters normally put a lower limit to the diffraction angle of 1–5 mrad. For X-rays of wavelength 0.15 nm the scattering objects are then smaller than 30 nm or at most 150 nm. The size, shape and orientation of these objects may be obtained from angular information in the SAXS pattern if point collimation is used. The scattered intensity from polymer fibres in SAXS is often very small, so with point collimation the divergence of the beam or the sample volume is increased in a compromise that reduces the pattern resolution. If a synchrotron source of X-rays is used, the extremely high brightness of the source allows very high-quality SAXS patterns to be obtained from a small bundle of fibres in 30 min. It is well known that a synchrotron source of X-rays allows new experiments, such as the real-time study of morphological changes[1–4]. We show here that apparently routine studies can also benefit.

The polymer materials studied are two versions of commercial poly(*p*-phenylene terephthalamide) fibre, Kevlar 49 and Kevlar 149. The more highly ordered Kevlar 149 has not previously been studied by SAXS. In both fibres the major feature in the SAXS pattern is a continuous monotonically decreasing streak along the equator. This is the major feature in many fibres, including high-modulus carbon fibres[5] and natural textile fibres. In some cases it is due to elongated voids in the fibre, and this has led to the name 'void scattering' being applied in all cases. Although the scattering only implies elongated regions of different electron density—better or worse packing of the molecules—the name sticks and can be misleading.

The intensity of SAXS from a sample containing two phases of different electron density ρ_1 and ρ_2 in volume fractions ϕ and $1-\phi$ depends on the product of two unknowns, $(\rho_1-\rho_2)$ and $\phi(1-\phi)$. Staining or swelling is often used to change the scattering, but these processes will affect the less ordered regions of the fibre as well as filling any accessible void. Thus ρ_1 (or ρ_2) changes but generally to another unknown. When voids become very small, of atomic dimensions, then a distribution of microvoids will be much the same as a disordered region with free volume, but one would not normally describe the amorphous regions of a semicrystalline polymer as containing voids. In the case of Kevlar 49 we will show that the scattering objects match the properties of the crystals, and there is no need to postulate any voids in the structure.

EXPERIMENTAL

The X-ray source for these studies was the Cornell High Energy Synchrotron Source (CHESS). The A-1 beam line was used, which has a wiggler magnet to increase the X-ray flux and a double-focusing monochromator. The result is a highly parallel beam of X-rays of wavelength 0.15 nm with a flux of 5×10^{11} photons s^{-1} in a 0.3×1 mm^2 spot at the detector plane. We used a 200 μm pinhole collimator to define the area of the sample that was being irradiated, and to remove parasitic scatter from earlier limiting slits. The beam had an axial or vertical divergence of about 1 mrad and a horizontal convergence of about 2 mrad. The sample-to-detector distance was 760 mm and the SAXS pattern was recorded on Kodak AA film. The diffraction patterns were scanned with a Joyce Loebl microdensitometer with a digital output. The microdensitometer slit used was 0.5×0.05 mm^2.

* To whom correspondence should be addressed
† Present address: IBM General Technology Division, Hopewell Junction, NY 12533, USA

0032-3861/91/071167-06

The digitized data were transferred to a Convex computer for further data analysis. Porod plots of the equatorial streak were made using $s^4I(s)$ and s^4 as the variables, where $s=2\sin\theta_B/\lambda$, $2\theta_B$ is the scattering angle and λ is the wavelength of the radiation, 0.15 nm. This formula is normally associated with unoriented samples, and a plot of $s^3I(s)$ vs. s^3 is more often used for well oriented fibres. This latter formula is correct for slit-collimated patterns, or for oriented patterns where a long microdensitometer slit captures all the intensity. The pattern here is point-collimated, and the slit length of 0.5 mm was much narrower than the width of the equatorial scatter. The angular width of the equatorial scatter was determined from the intensity scans perpendicular to the equatorial scatter at arbitrary values of $2\theta_B$. A third-order polynomial baseline was drawn to the data and the subtracted data set fit to a Gauss–Lorentz sum function using a non-linear least-squares fitting routine. The angular width was calculated from the fitted function as a full width at half-maximum (FWHM).

A limited amount of wide-angle X-ray diffraction (WAXD) was also performed on these fibres using a conventional source of Cu Kα radiation operating at 35 kV and 14 mA. The FWHM of the (0 0 4) and (0 0 6) reflections were measured with a Braun position-sensitive detector. A fibre bundle 0.7 mm thick was used as the sample. The sample-to-detector distance was 135 mm, and the collection time was 2 h. The FWHM was corrected for instrumental broadening using the FWHM of the (1 1 1) peak from copper foil and assuming a Gaussian lineshape. The apparent crystal size was determined by using the simple Scherrer equation, $L_{hkl}=K\lambda/(\text{FWHM})\cos\theta_B$ with $K=1$.

RESULTS AND DISCUSSION

We have used a sample of collagen from duck tendon to illustrate the comparison of SAXS from synchrotron and conventional X-ray sources. Collagen has a very well defined fibre structure, with a repeat distance along the fibre that varies from 60 to 68 nm depending on the condition of the sample[6]. The small-angle pattern consists of more than 20 meridional orders from this fibril periodicity. *Figure 1a* shows the SAXS pattern from this collagen sample recorded using a 12 kW rotating-anode generator. The exposure time needed was 21 h with a large Statton camera and a 380 μm collimator. *Figure 1b* is a SAXS pattern of the identical sample, but recorded at CHESS using a 200 μm collimator and an exposure time of 14 min. Clearly the reflections are better resolved in *Figure 1b* and the shape of the spot is no longer masked by beam divergence.

The rest of this paper is concerned, not with the naturally occurring collagen, but with a man-made high-performance fibre, poly(*p*-phenylene terephthalamide) (PPTA)[7,8], commercially available as Kevlar 29, Kevlar 49 and Kevlar 149 from DuPont. Well oriented semicrystalline fibre is formed by coagulation from a wet-spun nematic solution of PPTA. To improve the properties of the fibres, they are heat-treated under tension. Kevlar 29 and Kevlar 49 have been available for some time, and their structure–property relationships have been studied in detail[9–15]. Kevlar 149 was introduced more recently. It is essentially similar to the other types, but is heat-treated in a different manner. The density of Kevlar 149 is higher than that of Kevlar 49 and the water uptake is less, indicating a higher crystallinity[16]. It also has a 35% higher tensile modulus, 180 GPa, which is 80–90% of the theoretical modulus of 200–230 GPa[17].

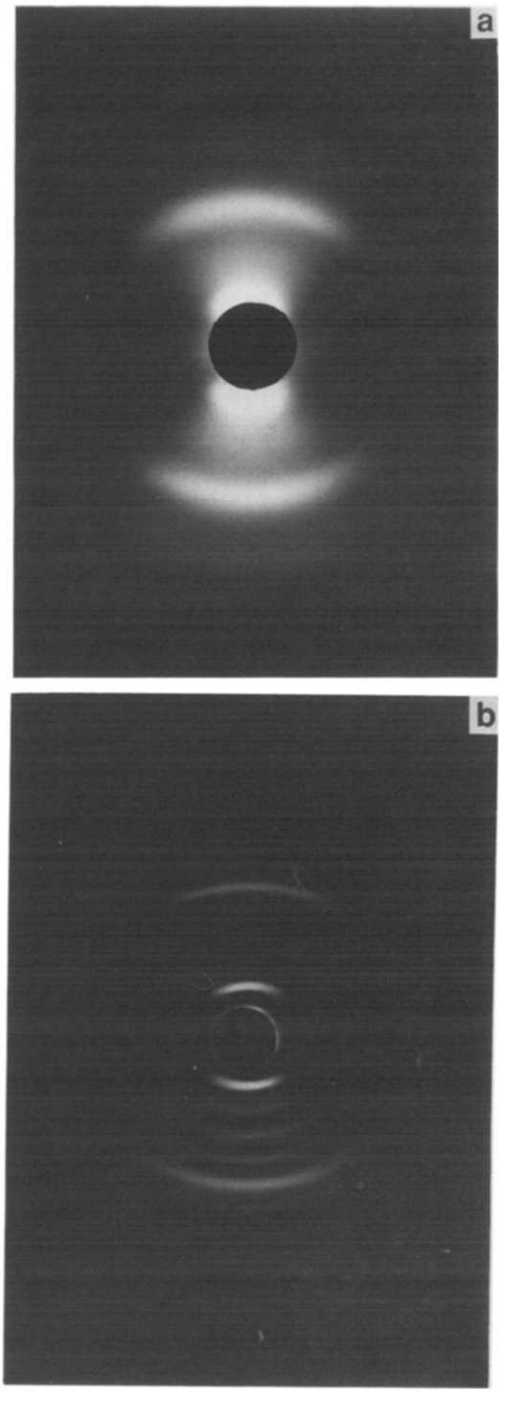

Figure 1 (a) SAXS pattern of duck tendon collagen recorded using a large Statton camera and a rotating-anode generator. (b) SAXS pattern of the same sample recorded at CHESS

Figure 2 shows the SAXS pattern of Kevlar 149 and *Figure 3* shows the SAXS pattern of Kevlar 49. The common feature is that the intensity in both is concentrated in a streak along the equator and there is nothing along the meridian. The streak has a fan-like structure increasing in width as the scattering angle $2\theta_B$ increases, as in carbon fibres[5]. The streak often appears triangular (*decreasing* in width as $2\theta_B$) in reproduction but this is due to the rapid fall in intensity as $2\theta_B$ increases, often combined with a large beam diameter. There are three

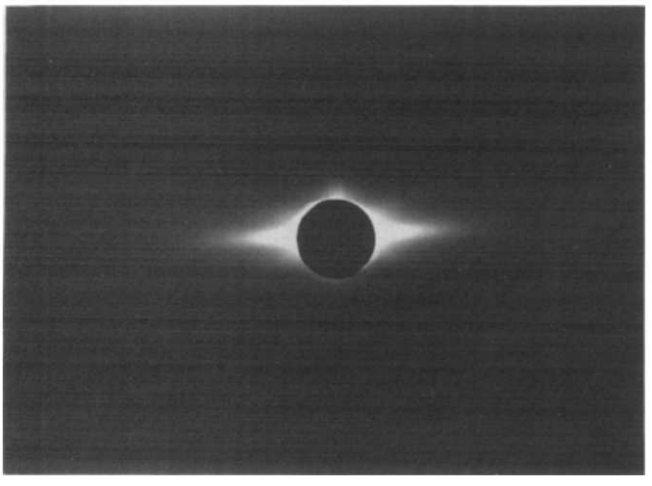

Figure 2 SAXS pattern of Kevlar 149

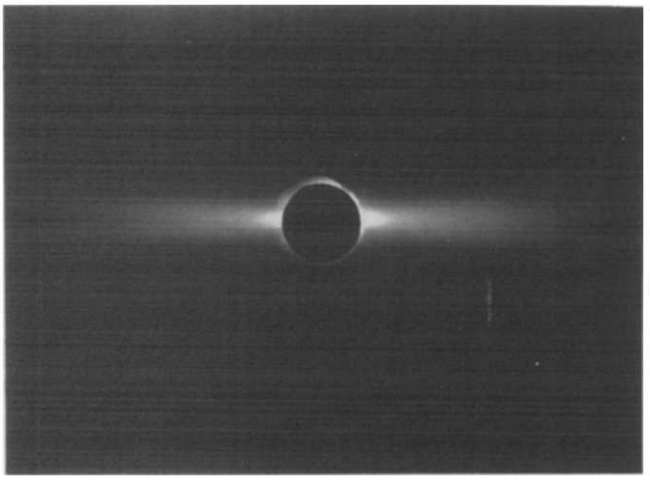

Figure 3 SAXS pattern of Kevlar 49

points of difference: compared to Kevlar 49, the scatter in Kevlar 149 is considerably weaker, it is concentrated closer to the central beam, and there is a pair of faint but clear off-axis streaks, at about $\pm 25°$ to the equator. These were not clearly visible in the best SAXS patterns that could be obtained with conventional X-ray sources.

The equatorial streak

An equatorial streak is produced by objects extended along the fibre direction, in the shape of needles or sheets. If the objects are perfectly aligned in the fibre direction and have a finite length L, then the angular width of the streak (measured in the direction of the fibre axis) will be a constant (λ/L). The observed increase in width with $2\theta_B$ is taken to be due to misorientation of these objects. In reciprocal space, the intensity distribution consists of the sum of a set of discs of thickness λ/L, with the disc normals misoriented from the fibre axis. It is then clear that, at large values of $2\theta_B$, the width should be proportional to $2\theta_B$ and the slope is the mean misorientation of the objects, ψ. At small values of $2\theta_B$ the width is λ/L (ref. 5). At intermediate values the widths of the two intensity distributions add. If both can be approximated to Gaussian form, then the resultant profile width is $[(\lambda/L)^2 + (2\theta_B\psi)^2]^{1/2}$.

To determine L and ψ the width of the equatorial streak was plotted vs. $2\theta_B$ and fitted to the function $(a+bx^2)^{1/2}$ using a non-linear least-squares fitting routine. The most important systematic error is inaccurate setting of the centre of the pattern, so the zero position of scattering angle was adjusted to improve the fit. The data were then replotted as the square of the angular width *versus* the square of the scattering angle, and refitted to a straight line. *Figures 4* and *5* show these plots for Kevlar 49 and Kevlar 149 respectively.

For Kevlar 49 the fit is good; the intercept at $\theta_B = 0$ corresponds to an object length of 65 nm and the slope $\psi^2 = 0.0714\,\text{rad}^2$ corresponds to a misorientation of 15.3°. A previous analysis[18] of SAXS from Kevlar 49 gave $\psi = 15.4°$. When the same procedure is used for Kevlar 149, the fit is not very good, and it gives a *negative* intercept. A much better fit is obtained when the data are limited to diffraction angles greater than 0.51°; the misorientation in Kevlar 149 is then 20° and the object length is 160 nm. There seems little justification for doing this in *Figure 5*, as the data at small scattering angles are compressed. *Figure 6* shows the same data in their original form, and the abrupt change of slope at scattering angles just above 0.5° is more visible. The values so far ignore the effect of the finite size of the beam at the detector plane. This is 0.7 mm, equivalent to $2\theta_B \approx 1$ mrad, or to an object 170 nm across. The beam profile could

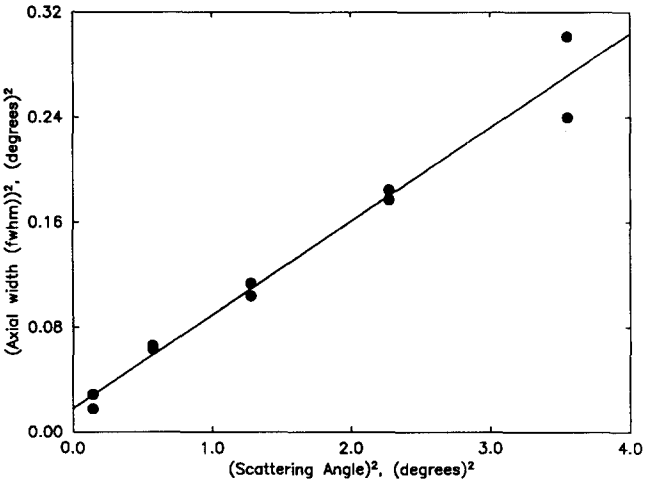

Figure 4 (Axial width)^2 of equatorial streak as a function of $(2\theta_B)^2$ for Kevlar 49

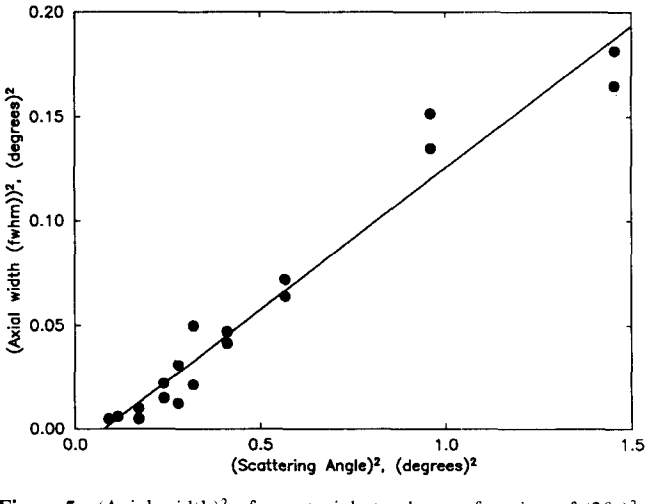

Figure 5 (Axial width)^2 of equatorial streak as a function of $(2\theta_B)^2$ for Kevlar 149

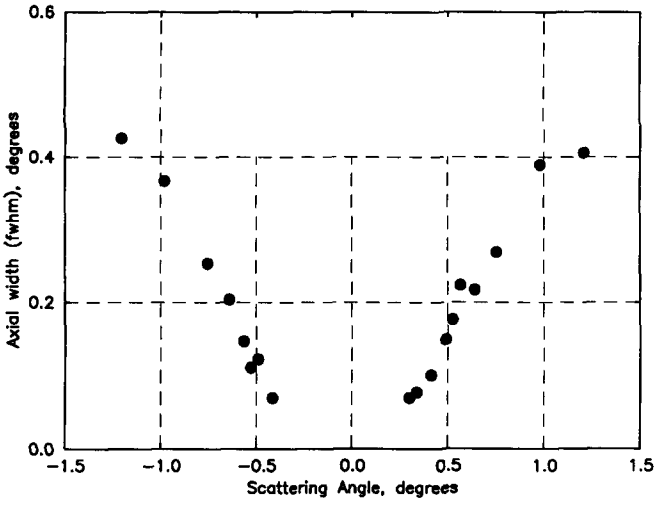

Figure 6 Axial width of equatorial streak as a function of $2\theta_B$ for Kevlar 149

not be determined accurately—overexposure was difficult to avoid. Assuming a Gaussian profile and correcting we get an object length of 70 nm for Kevlar 49 and 550 nm for Kevlar 149. There is only a small correction in the first case, so the uncertainty of the beam profile is not important. In the second case we can only say that the objects are large, over 200 nm long.

Fitting only one part of the data from Kevlar 149 implies that there are two distinct parts to the equatorial streak. The outer part at higher $2\theta_B$ was described above, so the size of >200 nm and misorientation of 20° correspond to objects of smaller lateral dimensions. What of the inner part of the streak? From *Figure 6* the curve is steeper at small values of $2\theta_B$, so it appears that the misorientation is greater. This is not correct, for a broader distribution would increase the width above its expected value. Instead there is a central well oriented streak, which causes the maximum intensity to rise as $2\theta_B$ falls. This causes the FWHM to fall rapidly, and it will not stabilize until the central sharp streak dominates the scattering. We do not have data at sufficiently small angles to be sure that we observe this. However, the observed width must always be greater than that of the central part of the streak and the minimum intercept at zero scattering angle corresponds to the size of the beam. A line through this intercept and the first few data points in *Figure 5* has a slope of 0.027, corresponding to a misorientation $\psi = 9°$. This is an upper limit to the misorientation when the scattering objects are very long. If they are as short as 200 nm, then their orientation is perfect, and $\psi = 4°$ when the length is about 350 nm.

The lateral size and distribution of the scattering objects control the distribution of intensity in the equatorial plane. Porod plots of $s^4I(s)$ vs. s^4 are shown in *Figures 7* and *8*. These have been used to obtain estimates of the density of interfaces whose normals lie in the equatorial plane. If the scattering objects are assumed to be cylindrical and to have a volume fraction of ϕ, then their size can be calculated from this interface density. The mean diameter of the scattering object $\bar{D}$ with these assumptions is given by:

$$\bar{D} = \frac{1}{2\pi^3(1-\phi)}\left(\frac{Q}{K}\right) \quad (1)$$

where $K = \lim_{s\to\infty}[s^4I(s)\,ds]$ and $q = 4\pi\int_0^\infty s^2I(s)\,ds$. This gives values of $1.6/(1-\phi)$ nm for Kevlar 49 and $4.4/(1-\phi)$ nm for Kevlar 149.

If ϕ is taken as the crystallinity of the sample (0.75 for Kevlar 49[19]; higher[16] for Kevlar 149, ≈ 0.8), the scattering objects are the crystalline fibrils and their widths are 6.4 nm for Kevlar 49 and ≈ 22 nm for Kevlar 149. If disordered regions or actual voids of lower concentration are taken as the scatterers, then the widths are 1.6–2.1 nm for Kevlar 49 and 4.4–5.5 nm for Kevlar 149.

Table 1 summarizes these SAXS results, and results from other authors on the size and orientation distribution of fibrous crystals in Kevlar, obtained by WAXD. We attempted to find the crystal length in Kevlar 149 by WAXD, using the breadth of meridional peaks. Proper separation of the effects of crystal size and crystal distortion by the method of Buchanan and Miller requires at least three orders of diffraction[20]. The lower orders are the more important for determining crystal size accurately. Unfortunately, only (0 0 4) and (0 0 6) gave good data, and we were unable to obtain a reliable breadth for the (0 0 2) reflection. *Table 2* gives the limited data obtained, in the form of apparent crystallite size L_{hkl}

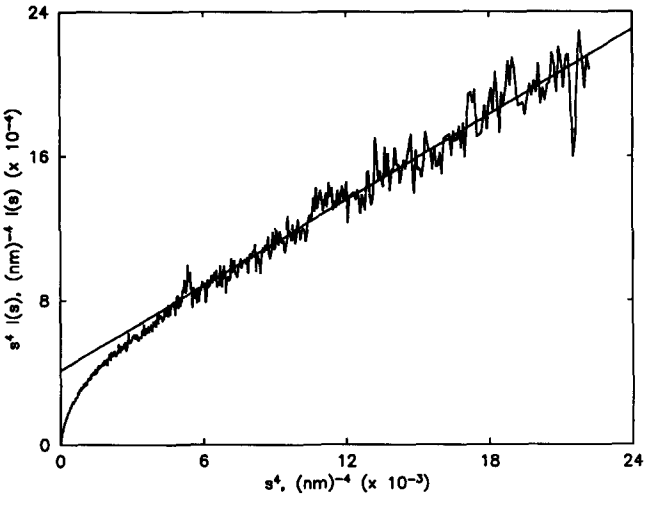

Figure 7 Equatorial intensity from Kevlar 49 plotted as $s^4I(s)$ vs. s^4 for Porod analysis

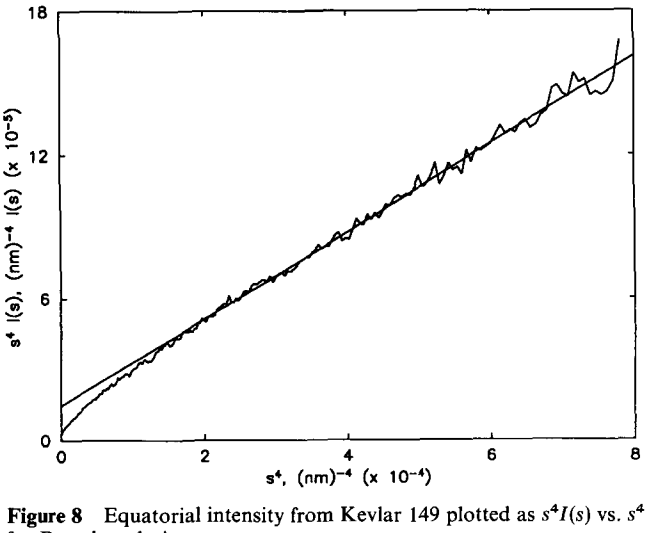

Figure 8 Equatorial intensity from Kevlar 149 plotted as $s^4I(s)$ vs. s^4 for Porod analysis

Table 1 Dimensions of scattering objects in Kevlar fibres

Fibre	Method	Orientation FWHM (deg)	Length (nm)	Width (nm)	
				Crystal	Void
Kevlar 49	SAXS	15.3	70	6.4	2
	WAXD	9.0[18], 14.8[19]	80[11,24]	4–5[16,19]	–
Kevlar 149	SAXS	20	>200	22	5
		<9	>200	–	–
	WAXD	4.2[23]	–	>10[16]	–

Table 2 Crystallite size (L_{hkl}) of Kevlar

Fibre	L_{004} (nm)	L_{006} (nm)
Kevlar 149	27	18
Kevlar 49	21	11
Kevlar 29	20	11

after correction for instrumental effects. Plotting $1/L$ vs. s^2, the intercept at $s=0$ should be 1/(crystallite length). For Kevlar 49 this length is the expected value of 80 nm. For Kevlar 149 the straight line through two data points gives a *smaller* length of ≈ 50 nm, difficult to believe.

The bimodal distribution of scattering objects in Kevlar 149 corresponds to the 'skin–core' structure suggested in some models for Kevlar, where the skin is more homogeneous and better ordered than the bulk of the fibre [11,21]. The misorientation of the major part of the SAXS streak is much larger than the WAXD misorientation of the crystals; the small inner streak could match but is not well enough defined to be certain of this.

Off-axis streaks

All that the existence of an off-axis streak in the SAXS pattern tells us is that there are oblique surfaces in the fibre. These surfaces have a well defined orientation, and at the surfaces the electron density changes. Since the scatter is weak, the surfaces are rare or the electron density difference is small (or both). It is not possible to determine the size of the objects causing the off-axis scattering, because of interference from the much stronger equatorial streak. There is no way to determine the nature of the scattering structure without additional information.

Kevlar 149 fibres were soaked in water overnight; the water is absorbed in disordered regions, decreasing the electron density difference between them and the crystallites. As expected, the equatorial scattering intensity decreased (note that this does not imply that voids have to be the cause of the scatter). The off-axis streaks became more visible; there was little change in their intensity. This indicates that the oblique interfaces are not simply a tilted population of the interfaces producing the equatorial streak, but much more information is needed.

In the 'radial pleated sheet' model for Kevlar 49 the molecules are arranged in sheets that extend longitudinally along the fibre axis and project radially outwards from the centre. These sheets contain the transverse intermolecular hydrogen bonds and they are not planar. They are pleated, having sharp changes of direction of about $\pm 10°$ every 300–500 nm along the fibre[12,13]. This should give rise to off-axis structure in SAXS, but none is seen in Kevlar 49. Both optical and X-ray observations show that the pleated sheet structure is not present in Kevlar 149 fibres; they have been straightened out and this improvement in orientation gives the increased modulus[17,22].

At this juncture we can only place the results in the context of other oriented polymer systems that produce off-axis SAXS intensity. In the case of polyethylene (PE), the unoriented polymer has a well defined lamellar structure on the scale of 10 nm and a ring in SAXS. Orientation causes this ring to become arced, and then to become two spots on the meridian as the lamellae break up and become aligned perpendicular to the draw direction. Heat treating drawn material can make the two spots split into four. The equilibrium orientation for the molecular chains is to pass through the lamellar crystal obliquely. On annealing, the molecular chains remain aligned along the draw direction and more perfect oblique lamellar surfaces are developed. These obliquely oriented crystals give rise to the off-axis spots. Electron microscopy of lamellar structures has confirmed this interpretation of the SAXS.

It is natural to try to apply the interpretation of this well understood case to Kevlar. It may not be correct, for when PE itself is well aligned and highly drawn to form a high-modulus fibre, the SAXS becomes a simple equatorial streak. Kevlar has no clear lamellar structure, but periodicities of 250–500 and 35 nm along the fibre have been observed[11–13] and the observed SAXS contains streaks, not well defined spots. In both Kevlar and PE the off-axis structure is seen after heat treatment, which increases the overall degree of order. In PE the spots are $\geqslant 45°$ from the equator and they are associated with oblique end surfaces of the crystals; in Kevlar 149 they are only 25° from the equator. Since the lattice spacing of PPTA along the fibre axis is 12.9 Å[10], compared to 2.54 Å for PE, low-index faces are much nearer the equator. For example (2 1 2) is a plane containing adjacent phenyl rings and 25° from the equator.

Recent experiments on other rigid-rod polymer fibres have shown that four-point off-axis SAXS patterns exist in heat-treated poly(bisbenzoxazole) (PBO) fibres but not in the as-spun fibre or in the chemically similar poly(bisbenzthiazole) (PBZT)[23]. These have only an equatorial streak and no meridional reflection. PBO even more than PPTA is a rigid-rod polymer; the chains have no flexibility at all. PBO is therefore very highly ordered and it is not expected to have any lamellar structure. Nevertheless it has a distinct four-point pattern and not four streaks. This has no explanation at present, and adds only uncertainty to interpretation of the result in Kevlar 149. The only common feature is that heat treatment brings out the off-axis structure whenever it appears.

ACKNOWLEDGEMENT

Two of the authors, D. T. Grubb and Keshav Prasad, are grateful to the National Science Foundation–Materials Science Center for financial support of this work.

REFERENCES

1 Riekel, C. 'Chemical Crystallography with Pulsed Neutrons and Synchrotron X-Rays' (Eds. M. A. Carrondo and G. A.

Jeffrey), NATO Advanced Study Institute Series C, Mathematical and Physical Sciences, Vol. 221, Reidel, Dordrecht, 1987, p. 443
2 Grubb, D. T. and Liu, J. J.-H. *J. Appl. Phys.* 1985, **58**, 2822
3 Grubb, D. T., Liu, J. J. H., Caffrey, M. and Bilderback, D. H. *J. Polym. Sci., Polym. Phys. Edn.* 1984, **22**, 367
4 Zachmann, H. G, Wu, W.-l. and Riekel, C. *Polym. Commun.* 1984, **25**, 76
5 Ruland, W. *J. Polym. Sci., Polym. Symp.* 1969, **28**, 143
6 Gathercole, I. J. and Keller, A. *Biochim. Biophys. Acta* 1978, **535**, 253
7 Black, W. B. in 'MTP International Review of Science, Physical Chemistry Series 2, Macromolecular Science', (Ed. C. E. H. Bawn), Butterworth, London, 1975, Ch. 2, p. 88
8 Ciferri, A. and Ward, I. M. (Eds.) 'Ultra-High Modulus Polymers', Applied Science, London, 1979
9 Tashiro, K., Kobayashi, M. and Tadakaro, H. *Macromolecules* 1977, **10**, 413
10 Northolt, M. G. *Eur. Polym. J.* 1974, **10**, 799
11 Panar, M., Avakian, P., Blume, R. C., Gardner, K. H., Gierke, T. D. and Yang, H. H. *J. Polym. Sci., Polym. Phys. Edn.* 1983, **21**, 1955
12 Dobb. M. G., Johnson, D. J. and Saville, B. P. *J. Polym. Sci., Polym. Phys. Edn.* 1977, **15**, 2201
13 Dobb, M. G., Johnson, D. J. and Saville, B. P. *J. Polym. Sci., Polym. Symp.* 1977, **58**, 237
14 Manabe, S., Kajita, S. and Kamide, K. *Seni-Kikai Gakkaishi* 1980, **33**, 54
15 Roche, E. J., Wolfe, M. S., Suna, A and Avakian, P. *J. Macromol. Sci.–Phys. (B)* 1985, **24**(1–4), 141
16 Riewald, P. G., Dhingra, A. and Chern, T. S. in Sixth International Conference on Composite Materials (Eds. Matthews, Buskell, *et al.*), 1987, p. 362
17 Krause. S. J., VeZie, D. L. and Adams, W. W. *Polym. Commun.* 1989, **30**, 10
18 Dobb, M. G., Johnson, D. J., Majeed, A. and Saville, B. P. *Polymer* 1979, **20**, 1284
19 Hindeleh, A. M. and Abdo, M. *Polymer* 1989, **30**, 218
20 Alexander, L. E. 'X-Ray Diffraction Methods in Polymer Science', Krieger, Malabar, FL, 1985
21 Li, L. S., Allard, L. F. and Bigelow, W. C. *J. Macromol. Sci.–Phys. (B)* 1983, **22**(2), 269
22 Allen, S. R. and Roche, E. J. *Polymer* 1989, **30**, 996
23 Adams, W. W. *et al.* to be published